# Characterization of Silicon Nanowire-based Pressure Sensors for Biomedical Applications

Sangwon Park[1], Heehun Kim[2]

1. Nano Science & Engineering, Yonsei University, Seoul 03722, Republic of Korea
2. Center for Nanomedicine, Institute for Basic Science (IBS), Seoul 03722, Republic of Korea

## Introduction



Fig.1| Illustration of pressure sensor placement upon bioelectronic gripper
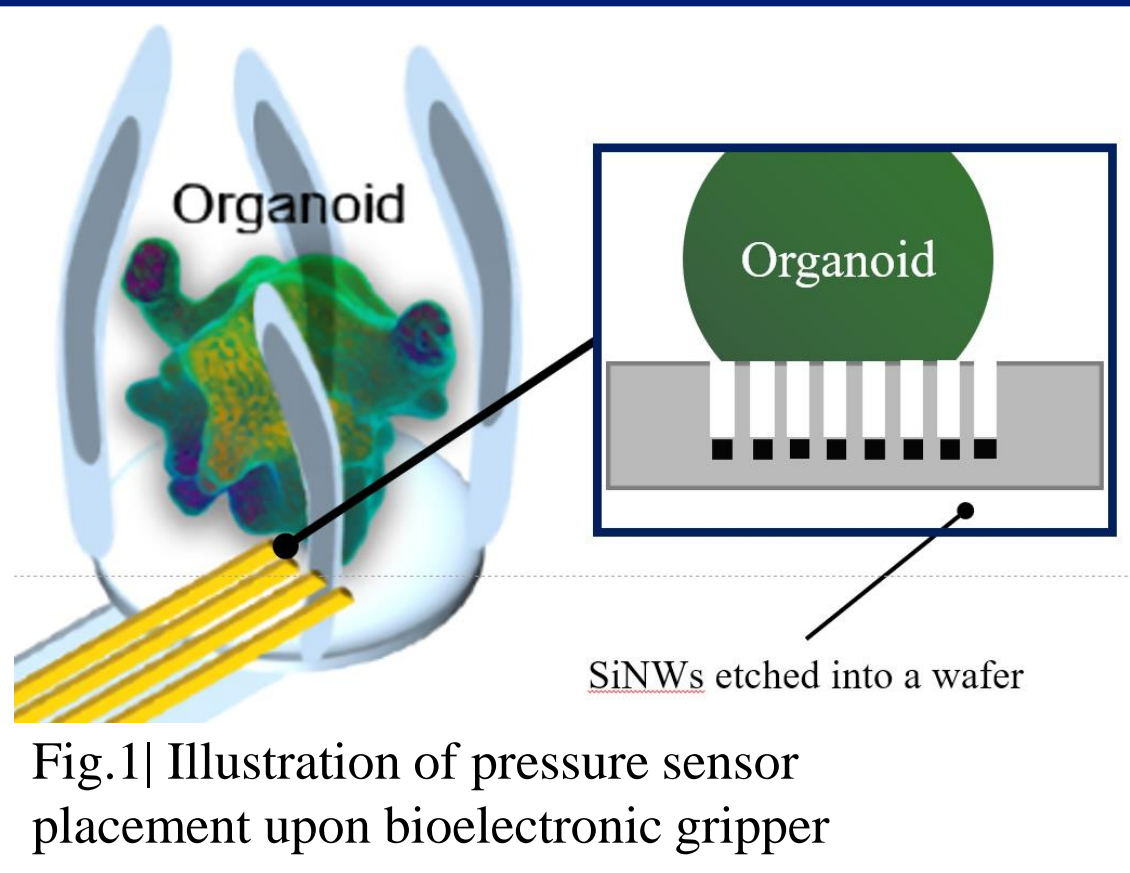
Recent advancements in bioelectronic grippers for electrophysiology research are focusing on active probes for stable, chronic neural recordings. These interfaces are actuated by external magnetic fields, and their controllability allows for adjusting gripping strength, reducing stress and ensuring the long-term stability of the neural recording interface. However, the issue lies with implementing a pressure sensor within the dimensional constraints of the probe (0.04mm$^2$ / thickness of 5um) and within fabrication limitations. The current hypothesis posits that employing a two-step MACE method using silver NP nanoparticles as an etching catalyst will yield effective SiNW structures, whose piezoresistive effects can be utilized for pressure sensors. The selected method integrates easily with conventional semiconductor manufacturing and doesn't interfere with subsequent processes. This research focuses on optimizing fabrication procedures for integrating SiNW-based pressure sensors into bioelectronic grippers and characterizing the PZR properties of SiNWs.

### Metal Assisted Chemical Etching MACE

**Dissolution Process**

Three process were proposed but none has been demonstrated to be the favorite.
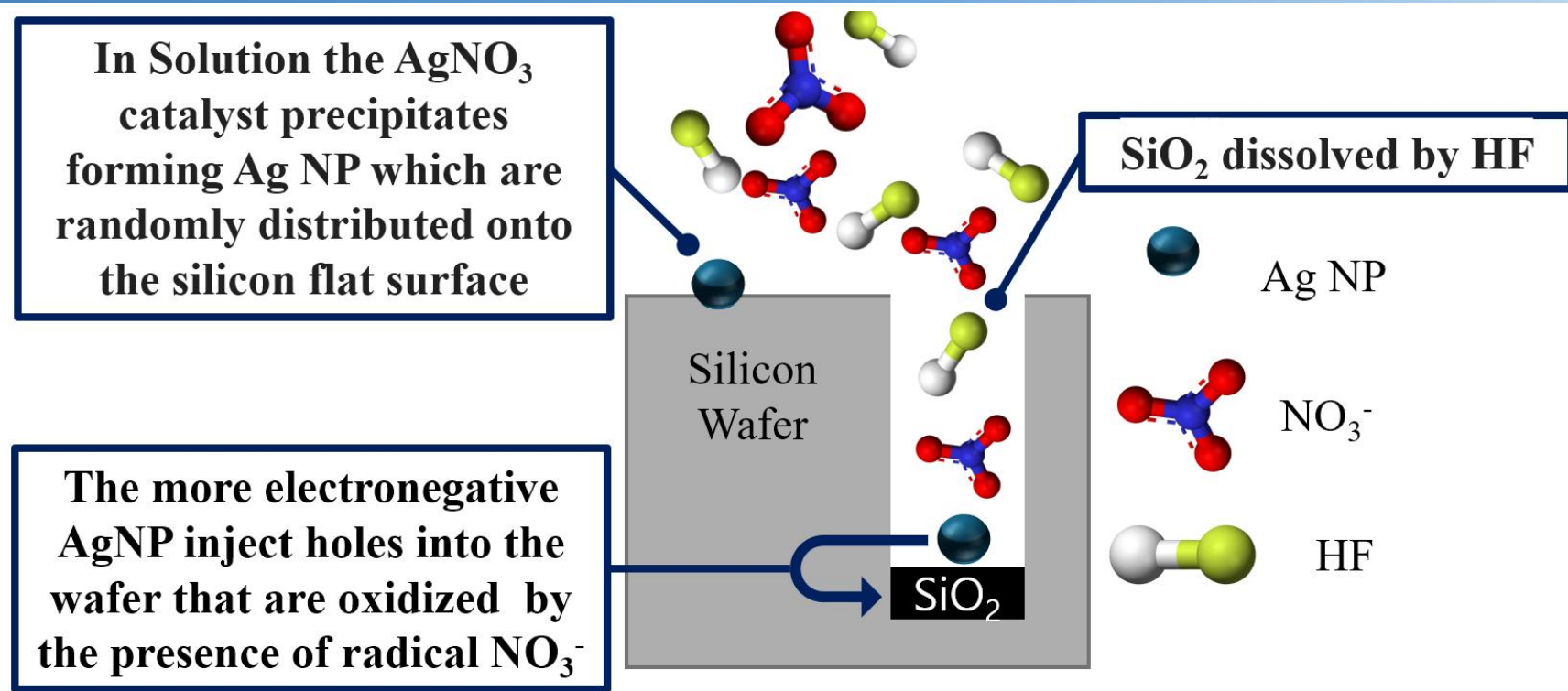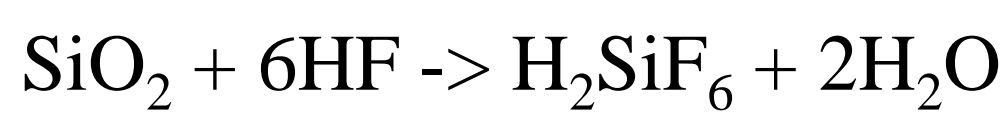<u>One example reaction:</u>

$$Si + 2H_2O \rightarrow SiO_2 + 4H^+ + 4e^-$$

$$SiO_2 + 6HF \rightarrow H_2SiF_6 + 2H_2O$$

In Solution the AgNO$_3$ catalyst precipitates forming Ag NP which are randomly distributed onto the silicon flat surface

SiO$_2$ dissolved by HF

Ag NP

NO$_3^-$

HF

The more electronegative AgNP inject holes into the wafer that are oxidized by the presence of radical NO$_3^-$

Fig.2 | Illustration of the MACE process

## Results

### 1. SEM image of SiNW cross section and surface area calculations

**0.04mm$^2$ area immersion bath**      **1cm$^2$ area selective etching**



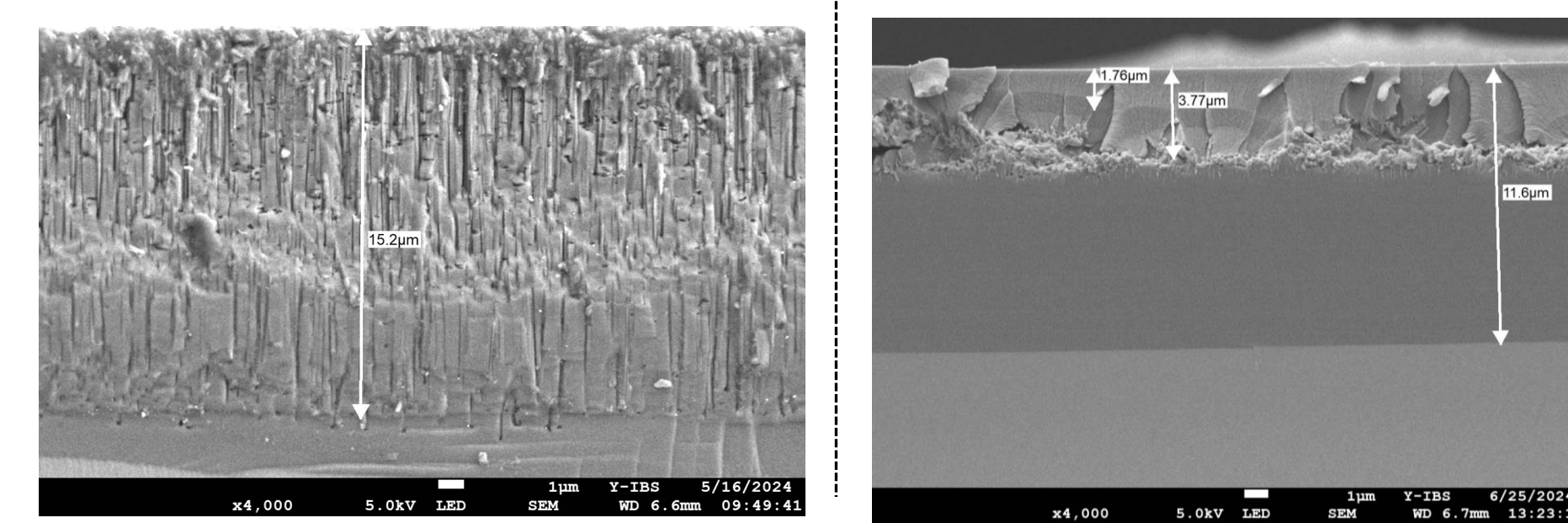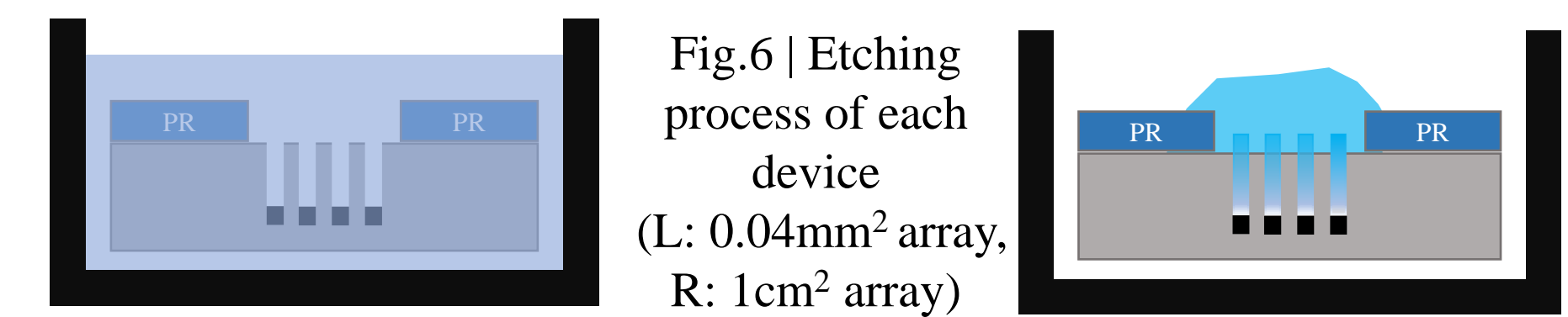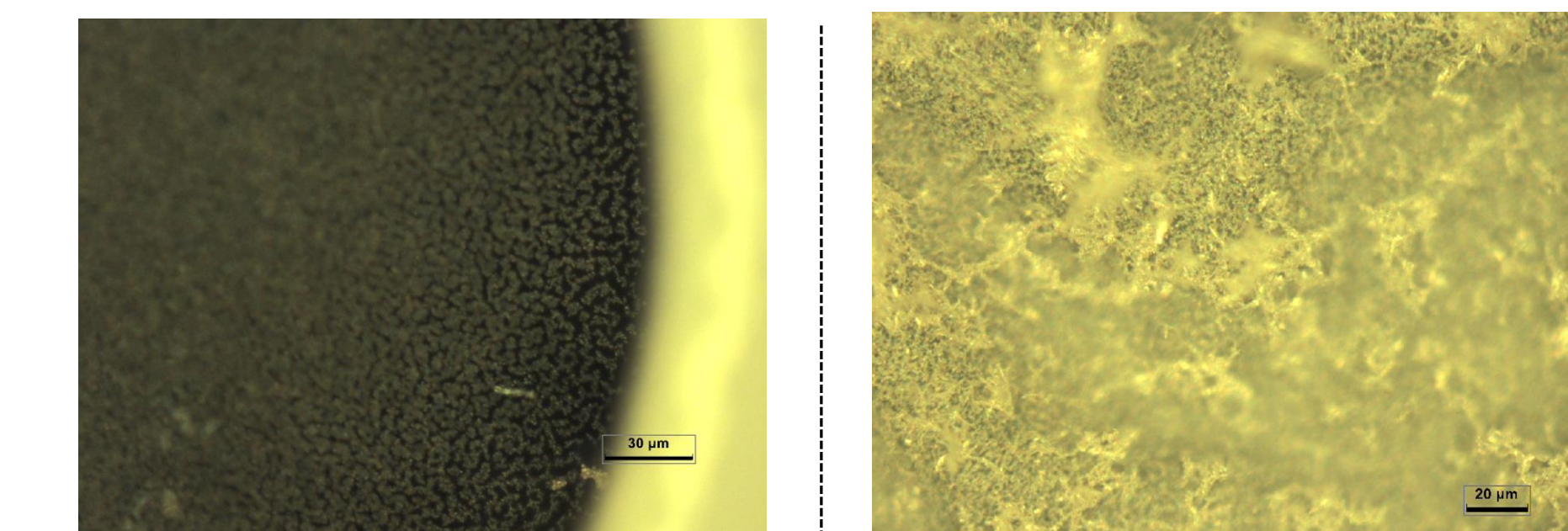Fig.6 | Etching process of each device (L: 0.04mm$^2$ array, R: 1cm$^2$ array)



Fig.7 | Cross sectional SEM view of SiNWs (L: 0.04mm$^2$ array, R: 1cm$^2$ array) Right sample is coated with a 3um layer of SU-8 for passivation.



Fig.8 | OM top view of SiNWs (L: 0.04mm$^2$ array, R: 1cm$^2$ array)

**Thickness Difference**: Wafer immersion in the etching solution resulted in SiNWs formation on the backside. For later attempts at measuring the piezoresistive constant, SiNWs produced by HF dripping were utilized.
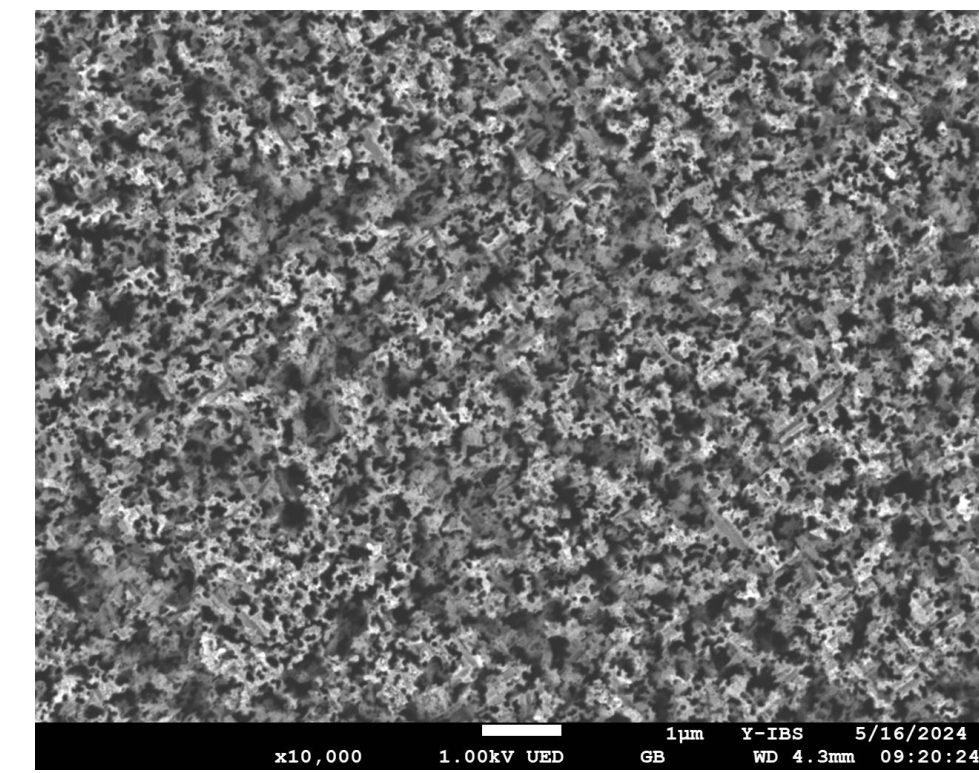


Fig.9 | Top-view of SEM image of SiNW

**Measuring Surface Area**: From the SEM image, Gwyddion was used to estimate the relative cross-sectional area of the SiNW to be <u>64.6%.</u>
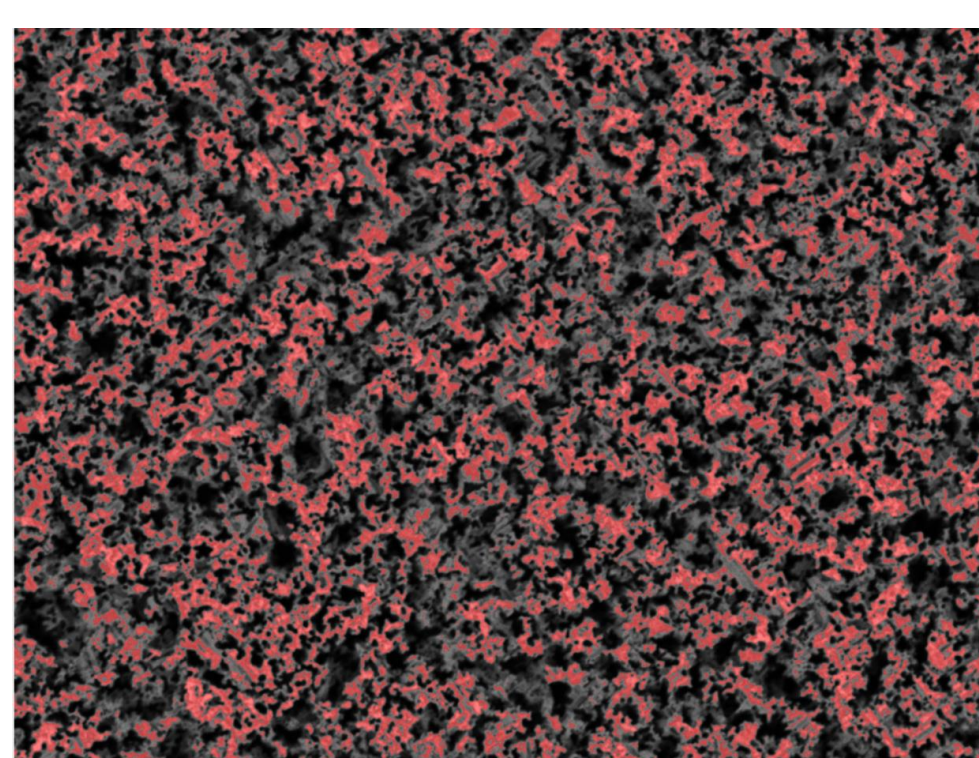


Fig. 10| Top-view of SEM image under Gwyddion Grain Analysis. Red areas are the tops of SiNWs.

### 3. Piezoresistance coefficient value calculations

To determine the piezoresistive coefficient multiple, repeated forces were applied to the SiNW, the subsequent resistance change graphed, and the change in resistance per unit area per given force were calculated than compared with literature.
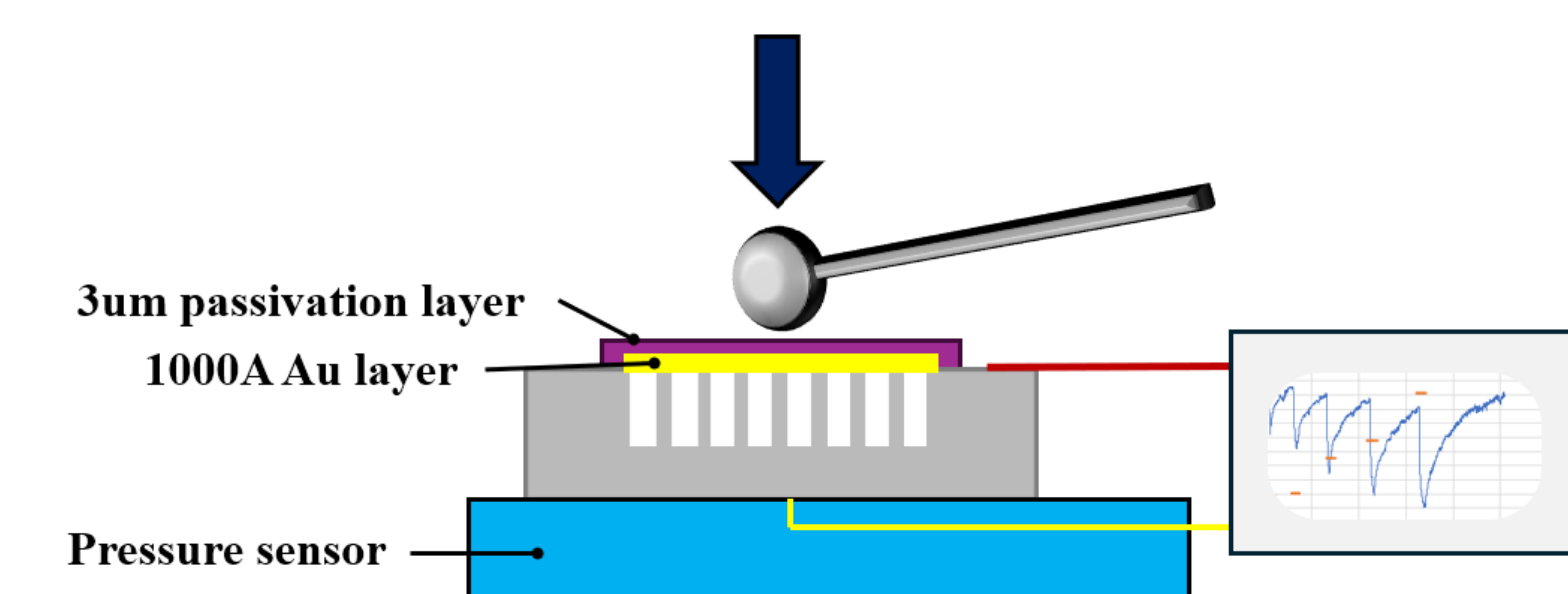


3um passivation layer
1000A Au layer
Pressure sensor

Fig.11 | Schematic of pressure load test. Compression made by pressing upon the passivation area using a Q-tip



Top          Bottom
SiNW area
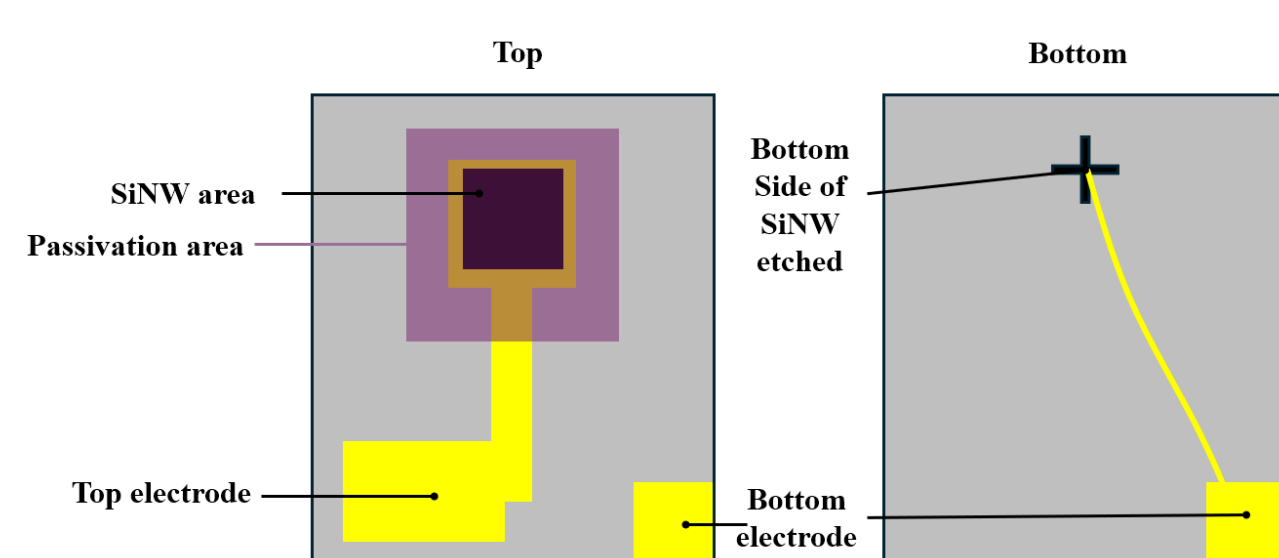Passivation area
Bottom Side of SiNW etched
Top electrode
Bottom electrode

Fig.12 | Top-view of SiNW pressure sensor for Piezoresistivity measurement



SiNW's response to repeated load-unload forces **(0.04mm$^2$ area)**



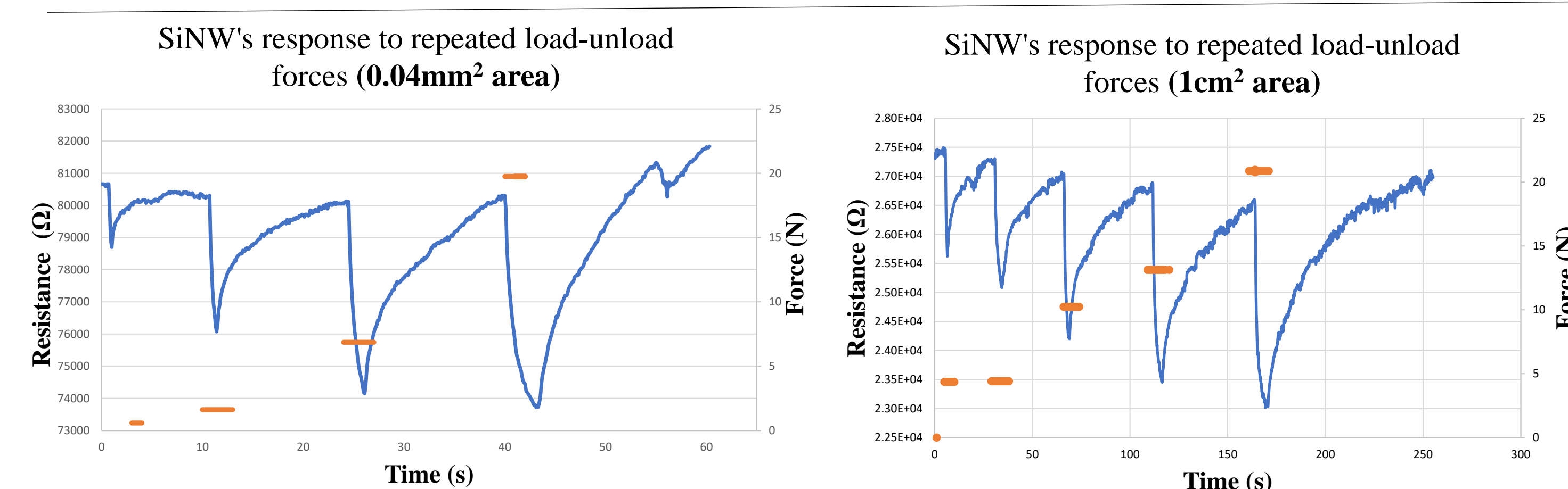SiNW's response to repeated load-unload forces **(1cm$^2$ area)**

Fig.13 | Change in resistance depending on specific force applied. (**Blue curve**: Resistance, **Orange curve**: Force)

## Experimental Methods



Etching Area Preparation          Ag NP Deposition          SiNW Etching          PR removal

SiO$_2$ layer Preparation          SiO$_2$ layer Deposition          PR removal          Gold Electrode Deposition          Passivation layer
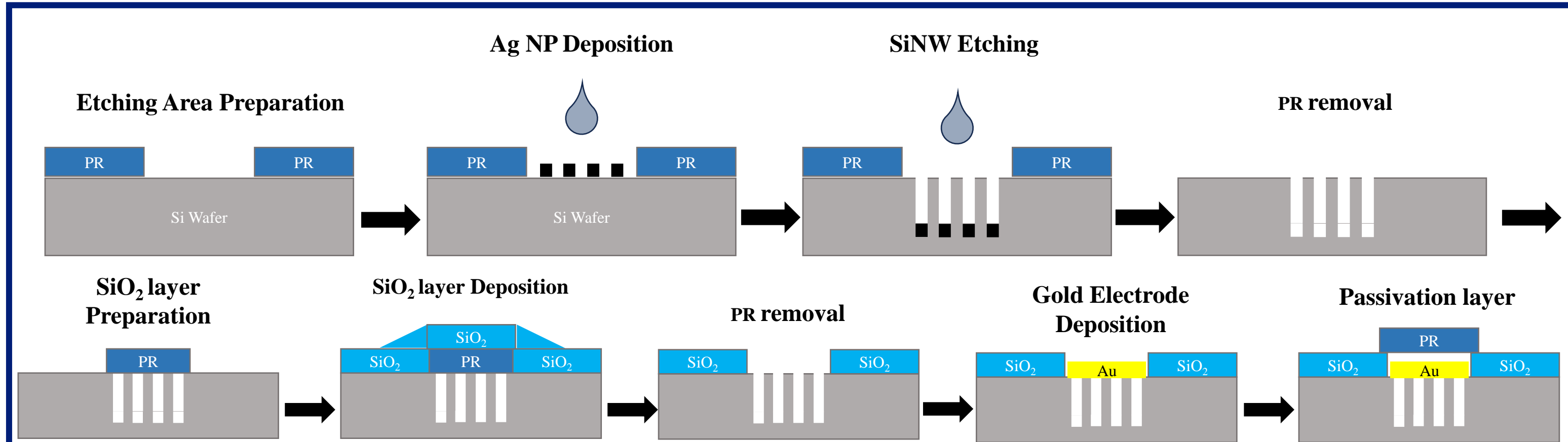
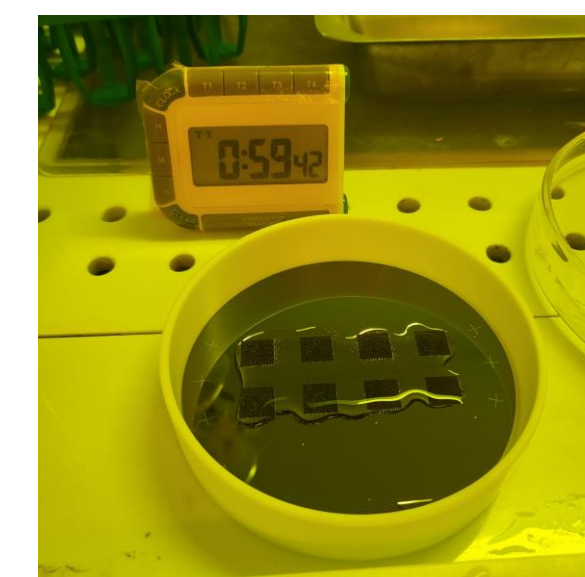Fig.3 | Device Fabrication Process in Cross Section View



Fig.4 | SiNW etching in progress, using drops of etchant.

**SiNW Etching:** 20% HF solution required to remove any natural oxide, Ag NP deposited by either immersing the wafer in 3M HF and 1.5mM of AgNO3 solution or dripping drops only onto the etching area using a spoid.
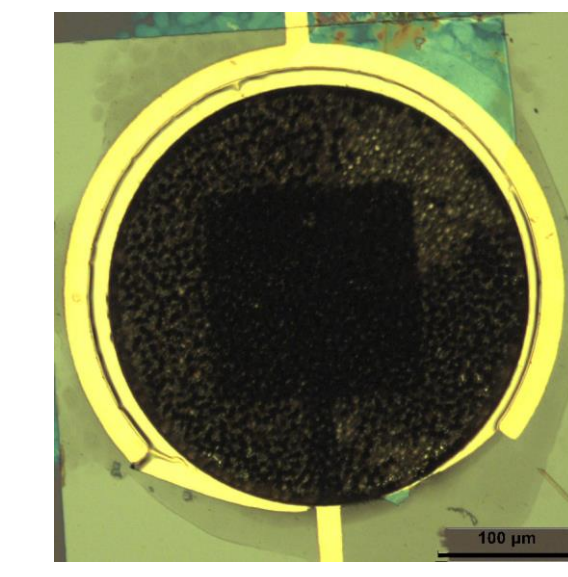


Fig.5 | Au Deposition results using RF Sputtering

**Gold Electrode Deposition:** Thermal evaporator used. Au deposition made using RF sputtering prove difficult to fully remove. AZ52124, AZP4620, DNR L300 all were unable to penetrate between the SiNWs.

### 3. Piezoresistance coefficient value calculations continued
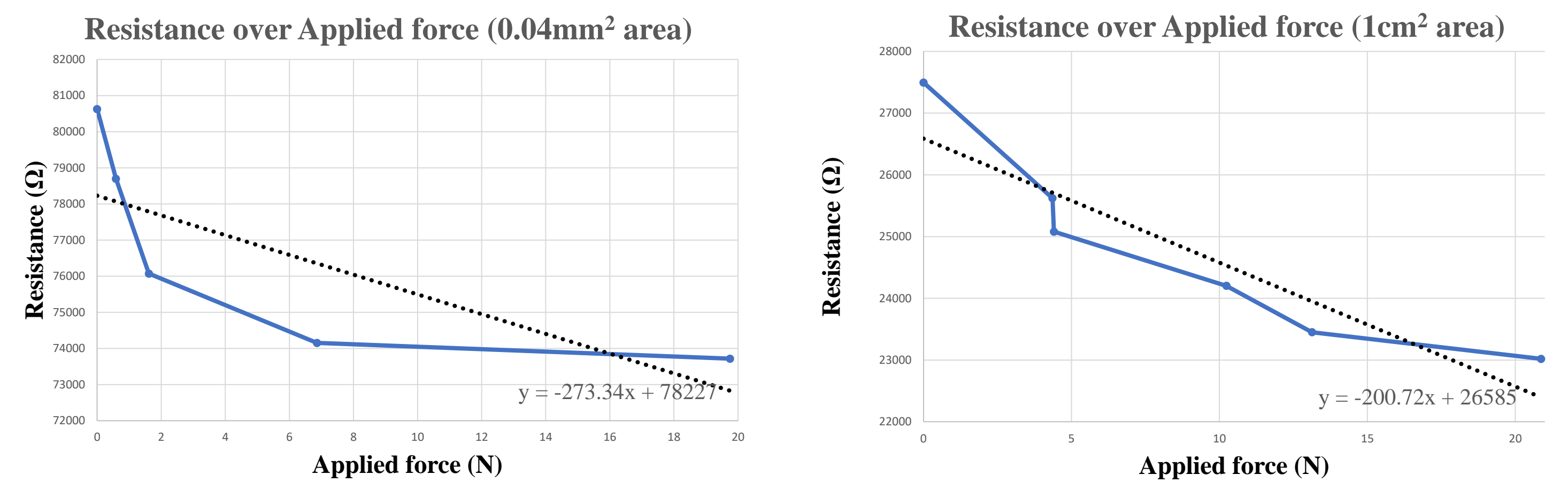


Resistance over Applied force (0.04mm$^2$ area)          $y = -273.34x + 78227$

Resistance over Applied force (1cm$^2$ area)          $y = -200.72x + 26585$

Fig.14 | Force Sensitivity of SiNW pressure sensor. $\Delta R$: -273.34 $\Omega$ / N (0.04mm$^2$), -200.72 $\Omega$ / N (1cm$^2$),

**Piezoresistance coefficient defined as**

$$\pi_l = \frac{\Delta \rho}{\rho_0} \frac{1}{X}$$

$\Delta\rho$: Stress-induced change in the resistivity
$\rho_0$: Reference resistivity
X: Stress

$$\pi_l = \frac{A_{NW}}{F} \times \frac{\Delta R}{R_0}$$

$A_{NW}$: Surface area of NW
F: Force applied in N
$\Delta R$: Change in resistance
$R_0$: Reference resistivity

| Piezoelectricity coefficient (Pa$^{-1}$) | |
|---|---|
| **0.04mm$^2$ area immersion bath mean** | **1cm$^2$ area selective etching mean** |
| -8.55 x 10-9 | -4.94 x 10$^{-7}$ |

Table 1 | Obtained Piezoelectricity coefficient values

**Value obtained from literature:**

$\sim 6 \times 10^{-6}$ Pa$^{-1}$

## Conclusion & Further Study

**Reasons for Piezoresistivity Coefficient Discrepancies**

- **0.04mm$^2$ area immersion bath**
  - Immersion in the etching solution resulted in SiNW forming on the backside of the wafer, which interfered with the results.

- **1cm$^2$ area selective etching**
  - The etching process appeared to halt prematurely, requiring constant refills. This likely resulted in SiNWs being etched too shallowly.

- **Both**
  - Accurate force application on the small area proved challenging, necessitating the use of a linear actuator.
  - The photoconductive effect influenced measurements: illumination of SiNWs with sufficient energy generated electron-hole pairs, increasing conductivity and affecting results.

**Fabrication Challenges**

- **Electrode Patterning on SiNWs**
  - Achieving precise electrode designs on SiNWs is difficult due to the need for photoresists with sufficient height and low viscosity to adequately cover the SiNWs.
  - These requirements have contradictory properties. Spin coating required meticulous attention, as SiNWs created "shadows" in the outer regions of the wafer, obstructing the spread of the photoresist.

**Further Studies:**

- Linear force gauge required for more accurate characterization of SiNW piezoresistivity
- Investigations into optimal fabrication techniques for PR coverage of SiNW's needed.

## Reference

[1] Fakhri, Elham, et al. "Piezoresistance characterization of silicon nanowires in uniaxial and isostatic pressure variation." Sensors, vol. 22, no. 17, 23 Aug. 2022, p. 6340, https://doi.org/10.3390/s22176340.
[2] Ghosh, Ramesh, et al. "Fabrication of piezoresistive SI nanorod-based pressure sensor arrays: A promising candidate for Portable Breath Monitoring Devices." Nano Energy, vol. 80, Feb. 2021, p. 105537, https://doi.org/10.1016/j.nanoen.2020.105537.
[3] Leonardi, Antonio Alessio, et al. "Silicon nanowires synthesis by metal-assisted Chemical Etching: A Review." Nanomaterials, vol. 11, no. 2, 3 Feb. 2021, p. 383, https://doi.org/10.3390/nano11020383.
[4] Milne, J. S., et al. "Giant piezoresistance effects in silicon nanowires and microwires." Physical Review Letters, vol. 105, no. 22, 23 Nov. 2010, https://doi.org/10.1103/physrevlett.105.226802.
[5] Muduli, Sakti Prasanna, et al. "Structural optimization of SI nanowires for ultimate efficiency improvement via tuning optical properties." Transactions on Electrical and Electronic Materials, vol. 24, no. 6, 23 Sept. 2023, pp. 489–501, https://doi.org/10.1007/s42341-023-00474-4.
[6] Rowe, A.C.H. "Piezoresistance in silicon and its nanostructures." Journal of Materials Research, vol. 29, no. 6, 28 Mar. 2014, pp. 731–744, https://doi.org/10.1557/jmr.2014.52.